Advances in Concrete Construction, *Vol. 9, No. 6 (2020) 577-588*
DOI: https://doi.org/10.12989/acc.2020.9.6.577

Effect of chiral structure for free vibration of DWCNTs: Modal analysis

Sehar Asghar[1], Muhammad N. Naeem[1], Mohamed Amine Khadimallah[2], Muzamal Hussain*[1], Zafar Iqbal[3,4] and Abdelouahed Tounsi[5,6]

[1]Department of Mathematics, Govt. College University Faisalabad, 38040, Faisalabad, Pakistan
[2]Prince Sattam Bin Abdulaziz University, College of Engineering, Civil Engineering Department, BP 655, Al-Kharj, 11942, Saudi Arabia
[3]Department of Mathematics, University of Mianwali, Punjab, Pakistan
[4]Department of Mathematics, University of Mianwali, Punjab, Pakistan
[5]Department of Civil and Environmental Engineering, King Fahd University of Petroleum & Minerals, 31261 Dhahran, Eastern Province, Saudi Arabia
[6]Materials and Hydrology Laboratory University of Sidi Bel Abbes, Algeria Faculty of Technology Civil Engineering Department, Algeria

(*Received April 7, 2020, Revised May 25, 2020, Accepted May 29, 2020*)

Abstract. In this paper, vibration attributes of chiral double-walled carbon nanotubes (CNTs) based on nonlocal elastic shell model have been investigated. The impact of small scale is being perceived by establishing Flügge shell model. The wave propagation is engaged to frame the ruling equations as eigen value system. The influence of nonlocal parameter subjected to different end supports has been overtly examined. A suitable choice of material properties and nonlocal parameter been focused to analyze the vibration characteristics. The new set of inner and outer tubes radii investigated in detail against aspect ratio and length. The dominance of boundary conditions via nonlocal parameter is shown graphically. Whereas for lower aspect ratio the frequencies coincide but as it continues to expand the difference between all respective boundary conditions slightly tend to increase. The results generated furnish the evidence regarding applicability of nonlocal shell model and also verified by earlier published literature.

Keywords: vibration; nonlocal parameter; double-walled CNTs; Flügge shell model

1. Introduction

The phenomenal development of nano science and nano technology is seen with an increase of its application in scientific research. Carbon nanotubes (CNTs) is such discovery by Iijima (1991) that may be used in a variety of fields like material reinforcement, aerospace, medicine, defense and microelectronic devices (Sosa *et al.* 2014, Soldano 2015, Fakhrabadi*et al.* 2015, Bouadi *et al.* 2018). Owing the striking mechanical properties through the cylindrical mechanism CNTs hold purposeful role in conveying fluid and gas. With a vast area of potential innovation, however CNTs demands more understanding to investigate its mechanical properties. Free vibration analysis of CNTs have been influential aspect in dynamical science for the last one decade. Vibration characteristics are investigated using thin shell theory by Yakobson *et al.* 1996), beam theory by Wang *et al.* (2006) and nonlocal beam theory (Zermi *et al.* 2015, Youcef *et al.* 2018).

An eminent study found in based upon ring theory by Vodenitcharova and Zhang (2003) whereas theories of continuum models developed by Li and chou (2003) in literature. Well known two main classes of models used to analyze the theoretical aspects of CNTs have been atomic model and other is continuum model. The classical molecular dynamics (MD) has shown to exceed those of other techniques such as ab initio and tight-binding MD included in class of atomic modeling (Iijima *et al.* 1996, Yakobson *et al.* 1997, Hernandez *et al.* 1998, Sanchez *et al.* 1999, Qian *et al.* 2002). The main reason continuum mechanics (Yoon *et al.* 2003, Fu *et al.* 2006, Ansari *et al.* 2011) turned noticeable tool is its computational capability to generate results of large range system in nanometer range. The nonlocal elasticity introduced by Eringen (1983, 2002) becomes a turning point as small scale effect was inculcated in to fundamental equations as simply material parameter. Therefore, scientific community now propose to apply nonlocal continuum models to investigate nano-structured materials (Sudak 2003, Wang *et al.* 2006, Pradhan and Phadikar 2009, Ansari *et al.* 2010, Hao *et al.* 2010, Amara *et al.* 2010, Shen and Zhang 2010). The first ever work presented on use of nonlocal elasticity was by Peddieson *et al.* (2003). Prominent computational competence and accuracy makes nonlocal models an attractive choice for further advancements in field. Donnell (1996) and Flügge (1962) have been two substantial shell theories practiced extensively in study of static and dynamic characteristics of CNTs. Flügge shell theory takes promising place to generate remarkably accurate developments to examine the CNTs. Dehsaraji *et al.* (2020) used higher-order shear and normal deformation theory to account thickness stretching effect for free vibration analysis of the cylindrical micro/nano shell subjected to an applied voltage and uniform temperature rising. Size

*Corresponding author, Ph.D.
E-mail: muzamal45@gmail.com,
muzamalhussain@gcuf.edu.pk

ISSN: 2287-5301 (Print), 2287-531X (Online)

dependency is included in governing equations based on the modified couple stress theory. Natuski and Qing *et al*. (2007) adopted wave propagation approach to investigate single- and double-walled CNTs brimming with fluids. Flügge shell theory was proposed to form governing equations of motion for CNTs. Arefi *et al*. (2019) studied the size dependent thermal buckling analysis of composite micro plate based on modified couple stress theory (MCST) and sinusoidal shear deformation theory. Arefi *et al*. (2019) studied the thermal and mechanical buckling analysis of micro plate reinforced with functionally graded (FG) graphene nanoplatelets based on modified strain gradient theory (MSGT Jamili *et al.* (2019) devoted to study post-buckling analysis of functionally graded carbon nanotubes reinforced composite (FG-CNTRC) micro plate with cut out subjected to magnetic field and resting on elastic medium. The basic formulation of plate is based on first order shear deformation theory (FSDT) and the material properties of FG-CNTRCs are presumed to be changed through the thickness direction. Rouhi and Ansari (2012) executed the axial buckling of double-walled CNTs subject to various layer-wise conditions by using Rayleigh-Ritz based upon nonlocal Flügge shell theory. Their study showed that the number of different layer-wise boundary conditions dominates the choice of values for nonlocal parameter. Dehsaraji *et al*. (2020) presented a new three-dimensional framework for thermo-electro-mechanical buckling analysis of functionally graded piezoelectric cylindrical nano/micro-shells subjected to axial mechanical compression, an external applied voltage and uniform temperature rising. To account thickness stretching effect, three-dimensional shear and normal deformation theory is employed. In another paper, Natuski *et al*. (2006) carried out the vibration analysis of nested CNTs in elastic matrix. Flügge shell theory again had been engaged to establish administrative shell equations while proposed method was wave propagation. Usuki and Yogo (2009) formed beam equations again based on Flügge shell theory, they concluded that if nonlocality and refined model are ignored then the generalized Beam theory and Flügge theory produce alike results. Arefi *et al*. (2019) presented the paper presents a large parametric investigation on the bending response of Functionally Graded (FG) polymer composite curved beams reinforced by graphene nanoplatelets resting on a Pasternak foundation. The theoretical framework is based on the First-order Shear Deformation Theory (FSDT) and the nonlocal elasticity theory. Sedighi (2020) performed the basis of finite element analysis, an eigenvalue problem to examine the vibrational characteristics of a hetero-nanotube made of carbon (C) and boron nitride (BN) nanotubes in magnetic and thermal environment. By incorporating the assumption of nonlocal elasticity theory, the size-dependent behavior of the considered structure is also taken into account. Further Wang and Zhang (2007) examined the bending and torsional stiffness of single-walled CNTs applying the Flügge shell equations. They presented three-dimensional model of single-walled CNTs in their work with effect of thickness. Arefi *et al*. (2018) applied a two-variable sinusoidal shear deformation theory (SSDT) and a nonlocal elasticity theory to analyze the free vibration behavior of functionally graded (FG) polymer composite nanoplates reinforced with graphene nanoplatelets (GNPs), resting on a Pasternak foundation Ansari and Rouhi (2013) summarized the effect of small scale, geometrical parameter and layer-wise end conditions of double-walled CNTs by adopting Flügge shell model (FSM).They depicted that the continuum model considering the nonlocal effect compels the short double-walled CNTs more flexible. Further Rouhi *et al*. (2015) worked on the multi-walled CNTs by developing nonlocal FSM and presented the frequency spectrum against layerwise boundary conditions. Recently Hussain and Naeem (2019a, b) performed the vibration of single-walled CNTs based on wave propagation approach and Galerkin's method. Arefi *et al*. (2016) presented an analytical method for the three-dimensional vibration analysis of a functionally graded cylindrical shell integrated by two thin functionally graded piezoelectric (FGP) layers. The first-order shear deformation theory is used to model the electromechanical system.

Salah *et al*. (2019) presented a simple four-variable integral plate theory for examining the thermal buckling properties of functionally graded material (FGM) sandwich plates. The proposed kinematics considers integral terms which include the effect of transverse shear deformations. Dehsaraji *et al.* (2020) studied the vibration analysis of functionally graded nanoshell based on the sinusoidal higher-order shear and normal deformation theory to account thickness stretching effect. To account size-dependency, Eringen nonlocal elasticity theory is used. For more accurate modeling the problem and corresponding numerical results, sinusoidal higher-order shear and normal deformation theory including out of plane normal strain. Zhang *et al*. (2018) studied an ultrathin flexible film but tends to buckle when subjected to compression and temperature variation. The buckling behavior will adversely affect its mechanical performance, therefore, it should be accurately evaluated and under controlled. Accordingly, it is vital to study thermal buckling behavior of ultrathin films. In the present work, thermal buckling of bilayer graphene sheets (GSs) embedded in Pasternak-type foundations is studied based on the nonlocal elastic theory.

In recent studies double-walled CNTs have been intensively attracted as that of single- walled CNTs due to its effectively applicable thermal, mechanical and electronic features. Hu *et al*. (2008) reported a study on the transverse and torsion waves based on nonlocal shell model for single-walled and double-walled CNTs. Xu *et al*. (2008) modeled the nested tubes of double-walled CNTs as separate elastic beam. Their work revealed that double-walled CNTs had no change for a particular invariable frequency subject to distinct edge conditions. Using nonlocal Timoshenko beam theory, Ke *et al*. (2009) investigated free nonlinear vibrations of double-walled CNT and applied differential quadrature technique to derive frequency equations. After wards Khosrozadeh and Hajabasi (2012) carried out vibration analysis of double-walled CNTs subject to nonlinear van der Waals forces. Aimed focus on values of nonlocal parameter, length of tube and surrounding elastic medium. Rouhi *et al.* (2013) adapted new numerical approach with nonlocal Donnell shell theory to inquire the small-scale effect on double walled-CNTs depending upon boundary conditions. Narwariya *et al.* (2018) presented the vibration and harmonic analysis of orthotropic laminated composite plate. The response of plate is determined using Finite Element Method. The eight noded shell 281 elements are used to analyze the orthotropic plates and results are obtained so that the right choice can be made in applications such as aircrafts, rockets, missiles, etc. to reduce the vibration amplitudes. Moreover, Benguidiab *et al.* (2014) explored the mechanical buckling features of zigzag double-walled CNT.A comprehensive research presented by Salvatore Brischetto (2015) to analyze the vibration characteristic of double-walled CNTs by considering shell continuum model. The findings of article were evolved around effects of van der Waals effect with regard to frequency ratio. Ayat *et al.* (2018) studied the use of optimum content of supplementary cementing materials (SCMs) such as limestone filler (LF) to blend with Portland cement such as increase in physical properties, enhancement of sustainability in concrete industry and reducing CO_2 emission are well known. Vibration analysis of chiral double-walled CNTs are rarely done in recent past. A limited number of researchers performed analysis first time to investigate the vibration of double-walled CNTs (Wang *et al.* 2006, Natuski *et al.* 2007, Shen and Zhang 2010, Ansari and Rouhi 2012, Ansari *et al.* 2013). So far as reviewed from the literature, vibration response of chiral double-walled CNT using wave propagation approach based on nonlocal FSM has not been investigated/assumed. Many material researchers calculated the frequency of CNTs using different techniques, for example, structural mechanics approach (Li and Chou 2003, Tahouneh 2017, Moradi and Payganeh 2017, Shafiei and Setoodeh 2017), shear deformation theory (Arefi *et al.* 2018, Lei and Zhang 2018), nonlocal continuum models (Sudak 2003, Wang *et al.* 2006, Pradhan and Phadikar 2009, Ansari *et al.* 2010, Hao *et al.* 2010, Amara *et al.* 2010, Shen and Zhang 2010, She *et al.* 2019), shell theory (Yakobson *et al.* 1996), beam theory (Wang *et al.* 2006), atomic modeling (Iijima *et al.* 1996, Yakobson*et al.* 1997, Hernandez *et al.* 1998, Sanchez *et al.* 1999, Qian *et al.* 2002), Rayleigh-Ritz (Ansari and Rouhi 2012), Galerkin method (Do *et al.* 2019) and axially loaded double beam system (Xiaobin *et al.* 2014). Moreover, the existing peculiar theoretical model contributes inventive numerical outputs for the vibration of CNTs as compare to prior models presented (Iijima *et al.* 1996, Qian *et al.* 2002, Peddison *et al.* 2003, Sudak 2003, Natuski *et al.* 2006, Shen and Zhang 2010, Ansari and Rouhi 2012, Yazdani and Mohammadimehr 2019, Sedighi and Yaghootian 2016, Sedighi *et al.* 2011, Behera and Kumari 2018, Batou *et al.* 2019, Zhang *et al*. 2018, Arefi *et al.* 2019, Arefi *et al*. 2019, Arefi *et al*. 2018, Arefi and Zenkour 2018).

The foremost intension of this paper to investigate vibrations characteristics of chiral double-walled CNTs by means of nonlocal elasticity shell model. The nonlocal shell model is established by inferring the nonlocal elasticity equations in to Flügge shell theory, which is our particular motivation. The suggested method to investigate the solution of fundamental eigen relations is wave propagation, which is a well-known and efficient technique to develop the fundamental frequency equations. It is carefully observed from the literature, no information is seen regarding present established model where such problem has been considered so it became an incentive to conduct current study. Whereas for lower aspect ratio the frequencies coincide but as it continues to expand the difference between all respective boundary conditions slightly tend to increase. The specific influence of four different end supports based on nonlocal FSM such as clamped-clamped (FSM-CC), clamped-simply supported (FSM-CS), simply supported-simply supported (FSM-SS) and clamped-free (FSM-CF) with assorted values of nonlocal parameter and distinguish inner tube radii are examined in detail.

2. Formation of nonlocal Flügge shell equations

Eringen (1983, 2002) acquainted the nonlocal elasticity theory as the stress on a given specific point x is a function of strain field at each point $x/$ in the body. This is how simply scale effect is treated as material parameter in fundamental equations of problem. On the other hand, because of unique dependence of stress state on strain state, classical elasticity cannot be useful for the scale effect. The basic expression in terms of the nonlocal stress tensor σ is written as follows (Eringen 1983, 2002)

$$\sigma(x)=\int_V \lambda(\left|x-x^{/}\right|,\mu)t(x^{/})dV(x^{/}).\forall x\varepsilon V \tag{1}$$

where $\lambda(|xx'|,\ \mu)$ stands for attenuation function/ nonlocal modulus with arguments as the Euclidean distance and t for macroscopic stress tensor. In $\mu = e_0 a/l$ as a is the interior distinctive length (length of C-C bond / lattice parameter / granular bond), l an exterior distinctive length (crack length/ wave length) and $e_o a$ be pertinent material parameter. The differential equivalent form of the equation 1 in two-dimension nonlocal elasticity theory can be written as

$$(1-(e_o a)^2\nabla^2)\sigma = t \tag{2}$$

The term $e_0 a$ describes the characteristic length known as nonlocal parameter. The stress and strain relationship is presented by generalized Hooke's law

$$t = S\colon \epsilon \tag{3}$$

Here S reads as fourth order elasticity tensor and ":" as double dot product.Thus, the relationship between stress and strain is expressed (Hussain and Naeem, 2019a, b).

$$\begin{Bmatrix}\sigma_{xx}\\ \sigma_{\theta\theta}\\ \sigma_{x\theta}\end{Bmatrix}-(e_o a)^2\nabla^2\begin{Bmatrix}\sigma_{xx}\\ \sigma_{\theta\theta}\\ \sigma_{x\theta}\end{Bmatrix}=\begin{pmatrix}\dfrac{E}{1-\nu^2} & \dfrac{\nu E}{1-\nu^2} & 0\\ \dfrac{\nu E}{1-\nu^2} & \dfrac{E}{1-\nu^2} & 0\\ 0 & 0 & \dfrac{E}{2(1-\nu^2)}\end{pmatrix}\begin{Bmatrix}\sigma_{xx}\\ \sigma_{\theta\theta}\\ \sigma_{x\theta}\end{Bmatrix} \tag{4}$$

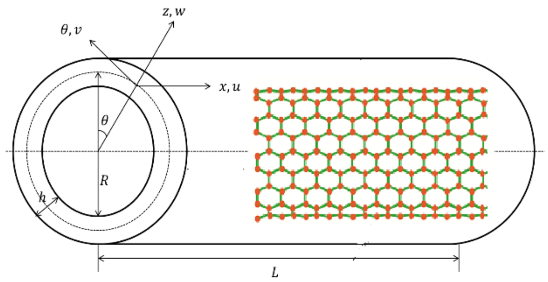

Fig. 1 A geometrical diagram of double-walled CNT

Here E symbolize as material's Young Modulus and v known as Poisson ratio.

The longitudinal and angular circumferential coordinates are shown by x and θ. Whereas σ_{xx}, $\sigma_{\theta\theta}$ and $\sigma_{x\theta}$ are normal and shear stress terms, ε_{xx}, $\varepsilon_{\theta\theta}$ and $\varepsilon_{x\theta}$ present the normal and shear strains .double-walled CNT comprised of two embedded tubes in which each tube is regarded as autonomous cylindrical shell assumes radius R, length L and thickness h shown in Fig. 1. The displacement components u_x, u_y and u_z in three directions x, θ and z according to classical shell theory are as (Hussain and Naeem 2019a, b)

$$u_x(x,\theta,z,t) = u(x,\theta,t) - z\frac{\partial w}{\partial x}(x,\theta,t) \tag{5a}$$

$$u_y(x,\theta,z,t) = v(x,\theta,t) - z\frac{\partial w}{\partial \theta}(x,\theta,t) \tag{5b}$$

$$u_z(x,\theta,z,t) = w(x,\theta,t) \tag{5c}$$

Where u, v and z signify surface displacements. The relations of middle surface strains and middle surface curvatures are symbolized as

$$\begin{aligned} &\varepsilon_{xx} = \frac{\partial u}{\partial x}, \varepsilon_{\theta\theta} = \frac{1}{R}\frac{\partial v}{\partial \theta} + \frac{w}{R}, \gamma_{x\theta} = \frac{\partial v}{\partial x} + \frac{1}{R}\frac{\partial u}{\partial \theta}, \\ &kxx = -\frac{\partial^2 w}{\partial x^2}, k_{\theta\theta} = -\frac{1}{R^2}\left(\frac{\partial^2 w}{\partial \theta^2} - \frac{\partial v}{\partial \theta}\right), \\ &k_{x\theta} = -\frac{2}{R}\left(\frac{\partial^2 w}{\partial \theta \partial x} - \frac{\partial v}{\partial x}\right) \end{aligned} \tag{6}$$

The kinematics expressions are written as

$$\begin{aligned} \varepsilon^o{}_{\theta\theta} &= \varepsilon_{\theta\theta} + zk_{\theta\theta} \\ \varepsilon^o{}_{xx} &= \varepsilon_{xx} + zk_{xx} \\ \gamma^o{}_{x\theta} &= \gamma_{x\theta} + zk_{x\theta} \end{aligned} \tag{7}$$

By utilizing stress factors in Eq. (4), stress resultant and moment resultant are derived and formulated in terms of kinematic relation in Flügge shell theory.

$$\begin{Bmatrix} N_{xx} \\ N_{\theta\theta} \\ N_{x\theta} \\ M_{xx} \\ M_{\theta\theta} \\ M_{x\theta} \end{Bmatrix} - (e_o a)^2 \begin{Bmatrix} N_{xx} \\ N_{\theta\theta} \\ N_{x\theta} \\ M_{xx} \\ M_{\theta\theta} \\ M_{x\theta} \end{Bmatrix} =$$

$$\begin{pmatrix} \frac{Eh}{1-\nu^2}\frac{\partial}{\partial x} & \frac{1}{R}\frac{\nu Eh}{1-\nu^2}\frac{\partial}{\partial \theta} & \frac{1}{R}\frac{\nu Eh}{1-\nu^2} \\ \frac{\nu Eh}{1-\nu^2}\frac{\partial}{\partial x} & \frac{1}{R}\frac{Eh}{1-\nu^2}\frac{\partial}{\partial \theta} & \frac{1}{R}\frac{Eh}{1-\nu^2} \\ \frac{1}{R}\frac{Eh}{2(1+\nu)}\frac{\partial}{\partial \theta} & \frac{Eh}{2(1+\nu)}\frac{\partial}{\partial x} & 0 \\ 0 & D\frac{\nu}{R^2}\frac{\partial}{\partial \theta} & -D\left(\frac{\partial^2}{\partial x^2} + \frac{\nu}{R^2}\frac{\partial^2}{\partial^2 \theta}\right) \\ 0 & D\frac{1}{R^2}\frac{\partial}{\partial \theta} & -D\left(\nu\frac{\partial^2}{\partial x^2} + \frac{1}{R^2}\frac{\partial^2}{\partial^2 \theta}\right) \\ 0 & \frac{D}{R}(1-\nu)\frac{\partial}{\partial x} & -\frac{D}{R}(1-\nu)\frac{\partial^2}{\partial \theta \partial x} \end{pmatrix} \begin{Bmatrix} u \\ v \\ w \end{Bmatrix} \tag{8}$$

Bending rigidity is presented by D and the fundamental equations are established on Flügge shell theory written as (Ansari and Arash 2013).

$$\begin{aligned} &\frac{\partial N_{xx}}{\partial x} + \frac{1}{R}\frac{\partial N_{x\theta}}{\partial \theta} = \rho h \frac{\partial^2 u}{\partial^2 t} \\ &\frac{1}{R}\frac{\partial N_{\theta\theta}}{\partial \theta} + \frac{\partial N_{x\theta}}{\partial x} + \frac{1}{R^2}\frac{\partial M_{\theta\theta}}{\partial \theta} + \frac{1}{R}\frac{\partial M_{x\theta}}{\partial x} = \rho h \frac{\partial^2 v}{\partial^2 t} \\ &\frac{\partial^2 M_{xx}}{\partial x^2} + \frac{1}{R^2}\frac{\partial^2 M_{\theta\theta}}{\partial^2 \theta} + \frac{2}{R}\frac{\partial^2 M_{x\theta}}{\partial \theta \partial x} - \frac{N_{\theta\theta}}{R} + p = \rho h \frac{\partial^2 w}{\partial^2 t} \end{aligned} \tag{9}$$

Where p denotes the exerted pressure on i tube through van der Waals (vdW) interaction forces. The proposed vdW model accounts the effects of interrelation force/pressure between the tubes of double-walled CNTs.

$$p = w_i \sum_{j=1}^{2} c_{ij} - \sum_{j=1}^{2} c_{ij} w_j \quad (i = 1, 2) \tag{10}$$

c_{ij} is vdW coefficient, depicting the pressure increment contributing from ith to jth tube.

$$c_{ij} = \left[\frac{1001\pi\varepsilon\sigma^{12}}{3a^4} E_{ij}{}^{13} - \frac{1120\pi\varepsilon\sigma^6}{9a^4} E_{ij}{}^{7}\right] R_j \tag{11}$$

Here C-C bond length is given by $a = 1.42\dot{A}$, depth of potential by ε, σ as parameter concluded by equilibrium distance, R_j as radius of j^{th} tube and $E_{ij}{}^m$ be as elliptic integral which is given as

$$E_{ij}{}^m = (R_j + R_i)^{-m} \int_0^{\pi/2} \frac{d\theta}{(1 - K_{ij}\cos^2\theta)^{m/2}} \tag{12}$$

being m as integer and coefficient K_{ij} is defined by

$$K_{ij} = \frac{4R_j R_i}{(R_j + R_i)^2} \tag{13}$$

By incorporating Eqs. (8) into (9), developed the set of partial differential equations written in terms of three field variables u^i, v^i, w^i (i=1,2) for the i^{th} tube of double-walled CNTs.

$$\begin{aligned} &g_{11}{}^{(1)}u^1 + g_{12}{}^{(1)}v^1 + g_{13}{}^{(1)}w^1 = \\ &\rho h\left(\ddot{u}^{(1)} - (e_o a)^2\left(\ddot{u}^{(1)}_{xx} + \frac{1}{R_1^2}\ddot{u}^{(1)}_{xx}\right)\right) \end{aligned} \tag{14a}$$

$$g_{21}{}^{(1)}u^1+g_{22}{}^{(1)}v^1+g_{23}{}^{(1)}w^1= \rho h\left(\ddot{v}^{(1)}-(e_oa)^2(\ddot{v}^{(1)}_{xx}+\frac{1}{R_1^2}\ddot{v}^{(1)}_{xx})\right) \tag{14b}$$

$$g_{31}{}^{(1)}u^1+g_{32}{}^{(1)}v^1+g_{33}{}^{(1)}w^1= \rho h\ddot{w}^{(1)}+w^{(1)}\sum_{\substack{j=1\\j\neq i}}^{2}c_{1j}-\sum_{\substack{j=1\\j\neq i}}^{2}c_{1j}w^{(j)}- (e_oa)^2\left[\begin{matrix}\rho h(\ddot{w}^{(1)}_{xx}+\frac{1}{R_1^2}\ddot{w}^{(1)}_{\theta\theta})+(\ddot{w}^{(1)}_{xx}+\\ \frac{1}{R_1^2}\ddot{w}^{(1)}_{\theta\theta})\sum_{\substack{j=1\\j\neq i}}^{2}c_{1j}-\sum_{\substack{j=1\\j\neq i}}^{2}c_{1j}(\ddot{w}^{(j)}_{xx}+\frac{1}{R_1^2}\ddot{w}^{(j)}_{\theta\theta})\end{matrix}\right] \tag{14c}$$

$$g_{11}{}^{(2)}u^2+g_{12}{}^{(2)}v^2+g_{13}{}^{(2)}w^2= \rho h\left(\ddot{u}^{(2)}-(e_oa)^2(\ddot{u}^{(2)}_{xx}+\frac{1}{R_2^2}\ddot{u}_{\theta\theta}{}^{(2)})\right) \tag{14d}$$

$$g_{21}{}^{(2)}u^2+g_{22}{}^{(2)}v^2+g_{23}{}^{(2)}w^2= \rho h\left(\ddot{v}^{(2)}-(e_oa)^2(\ddot{v}^{(2)}_{xx}+\frac{1}{R_2^2}\ddot{v}^{(2)}_{xx})\right) \tag{14e}$$

$$g_{31}{}^{(2)}u^2+g_{32}{}^{(2)}v^2+g_{33}{}^{(2)}w^2= \rho h\ddot{w}^{(2)}+w^{(2)}\sum_{\substack{j=1\\j\neq 2}}^{2}c_{2j}-\sum_{\substack{j=1\\j\neq 2}}^{2}c_{2j}w^{(j)}- (e_oa)^2\left[\begin{matrix}\rho h(\ddot{w}^{(2)}_{xx}+\frac{1}{R_2^2}\ddot{w}^{(2)}_{\theta\theta})+(\ddot{w}^{(2)}_{xx}+\\ \frac{1}{R_2^2}\ddot{w}^{(2)}_{\theta\theta})\sum_{\substack{j=1\\j\neq 2}}^{2}c_{2j}-\sum_{\substack{j=1\\j\neq 2}}^{2}c_{2j}(\ddot{w}^{(j)}_{xx}+\frac{1}{R_2^2}\ddot{w}^{(j)}_{\theta\theta})\end{matrix}\right] \tag{14f}$$

where g_{pq}=(p,q=1,2,3) serve as the partial operators and can be seen in Appendix-I.

3. Solution using the wave propagation approach

Over the past several years, many theories of vibration of tube/shell structures of various configurations and boundary conditions have been extensively studied (Iijima *et al.*1996, Natuski *et al.* 2006, Shen and Zhang 2010, Ansari and Rouhi 2012). One of the major numerical techniques is the wave propagation that is broadly and effectively applied by researchers to perform the free vibrations of single-walled CNTs problems (Hussain and Naeem 2019a)..The three modal displacement functions of the shell for ith tube can be regarded as

$$u^{(i)}(x,\theta,t)=a_m\cos(n\theta)e^{(i\omega t-ik_mx)} \tag{15a}$$

$$v^{(i)}(x,\theta,t)=b_m\sin(n\theta)e^{(i\omega t-ik_mx)} \tag{15b}$$

$$w^{(i)}(x,\theta,t)=c_m\cos(n\theta)e^{(i\omega t-ik_mx)} \tag{15c}$$

The displacement amplitude in x, θ and z directions are defined by a_m, b_m, c_m respectively. Angular frequency is denoted by ω, circumferential wave number by n and k_m regarded as axial wave number related with end supports imposed on double-walled CNTs. On substituting the functions and derivatives into the field equations, hence obtained a new group of coeval equations as follows

$$G_{11}{}^{(i)}a^i_m+G_{12}{}^{(i)}b^i_m+G_{13}{}^{(i)}c^i_m= -\omega^2\left(1-(e_oa)^2\nabla^2\right)\rho ha^i_m \tag{16a}$$

$$G_{21}{}^{(i)}a^i_m+G_{22}{}^{(i)}b^i_m+G_{23}{}^{(i)}c^i_m= -\omega^2\left(1-(e_oa)\nabla^2\right)\rho hb^i_m \tag{16b}$$

$$G_{31}{}^{(i)}a^i_m+G_{32}{}^{(i)}b^i_m+G_{33}{}^{(i)}c^i_m+ \left(1-(e_oa)^2\nabla^2\right)\left[\sum_{\substack{j=1\\j\neq i}}^{2}c_{ij}c^i_m-\sum_{\substack{j=1\\j\neq i}}^{2}c_{ij}c^i_m\right]= -\omega^2\left(1-(e_oa)^2\nabla^2\right)\rho hc^i_m \tag{16c}$$

Where i=(1,2) and the algebraic operators $G^{(i)}_{pq}$ are derived using Appendix-II with p,q=(1,2,3). The frequency vibration of double-walled CNT is exhibited based on nonlocal FSM subject to four end supports clamped-clamped (FSM-CC), clamped-simply supported(FSM-CS), simply supported-simply supported (FSM-SS) and clamped-free (FSM-CF).

4. Results and discussion

In this portion of writing, the significance of boundary conditions on the vibration behavior of double-walled CNT is investigated employing wave propagation approach. The versatility and accuracy of proposed method is seen by numerous studies (Natuski*et al.* 2006, Natuski *et al.* 2007) to determine natural frequencies in shell and CNTs. This study specifically scrutinizes the small scale effect in the vibration analysis of double-walled CNT. The numerical values of Young modulus, Poisson's ratio, thickness and density are E=1 TPa, ν=0.3, h=0.34 nm and ρ=2.3 g/cm^3 reported (Ansari and Arash 2013). Moreover, distinguished values of inner tube radius together with nonlocal parameter signifies the present nonlocal shell-based model to analyze frequency spectra. CNT is well known structure in shapes of i) armchair ii) chiral and iii) zigzag, herethe vibration analysis is carried out of zigzag CNT subjected to four

Table 1 Comparison of FSM double-walled CNT frequencies with Loy *et al*. (1999)

L/R	h/R	Method	N					
			1	2	3	4	5	6
20	0.01	Loy *et al*. (1999)	0.016102	0.009382	0.022105	0.042095	0.06801	0.09973
		FSM	0.016101	0.009378	0.022103	0.042094	0.04209	0.09973

Table 2 FSM frequencies of clamped double-walled CNTs (h/R=0.05, L/R=2.5)

m	V	N	Heydarpour *et al.* (2014)	Present
		7	0.6240	0.6228
	0.12	9	0.6240	0.6234
		11	0.6240	0.6239
		7	0.8157	0.8143
0	0.17	9	0.8157	0.8152
		11	0.8157	0.8155
		7	0.8553	0.8541
	0.28	9	0.8553	0.8547
		11	0.8553	0.8550

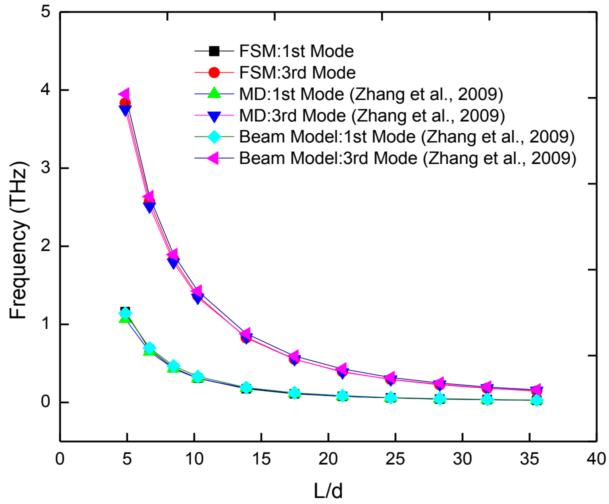

Fig. 2 Frequency comparison of FSM-CC double-walled CNTs for 1st and 3rd mode against L/d with FSM and MD simulations (Zhang *et al.* 2009)

conditions FSM-CC,FSM-CS,FSM-SS and FSM-CF. For the convergence rate of CNT, the non-dimensional frequency parameters enumerated in the current work, i.e., using FSM, are happened to be in a good consistency along with the so-called exact results furnished by Loy *et al.* (Loy 1999), those were established by working out with the deformation theory provided in Table 1. The Frequencies are described for non-dimensional frequency parameters as: $\xi = \omega R\sqrt{(1-\nu^2)\rho / E}$ as shown in Table 1 and positive coherence is achieved. The percentage difference is negligible as n=1,3,4 are 0.006%, 0.01%, 0.002% and at n=2 by 0.0061% and present FSM result are lower than equivalent results executed by Loy *et al.* (1999). The frequency parameters for circumferential wave numbers n=5, 6 are same with the outcomes of Loy *et al.* (1999). A non-dimensional frequency parameter ξ is defined for a

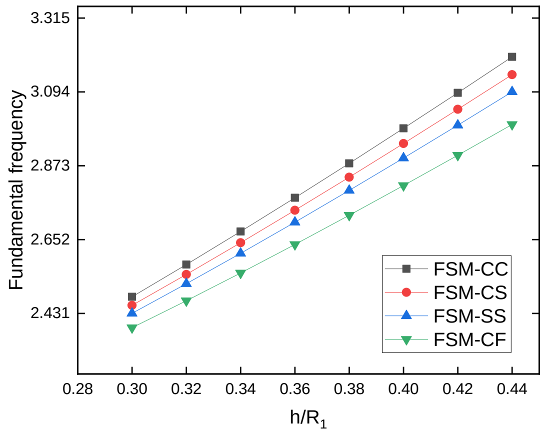

(a) against nonlocal parameter e_0a=0.18 with R_1=0.35 nm

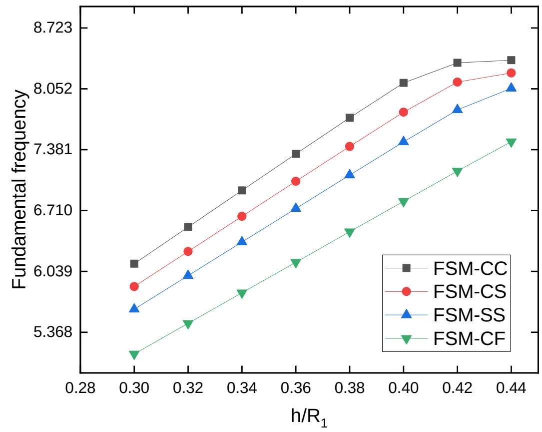

(b) against nonlocal parameter e_0a=0.18 with R_1=1.5 nm

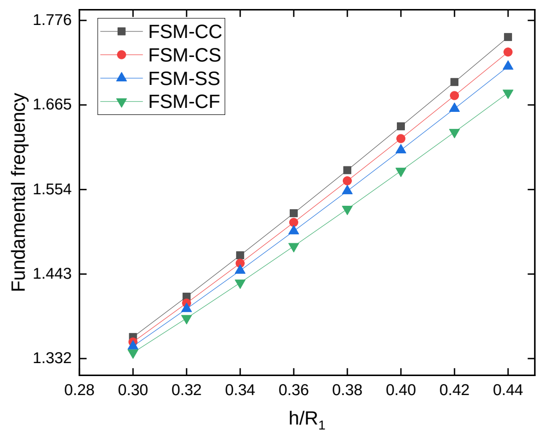

(c) against nonlocal parameter e_0a=0.40 with R_1=0.35 nm

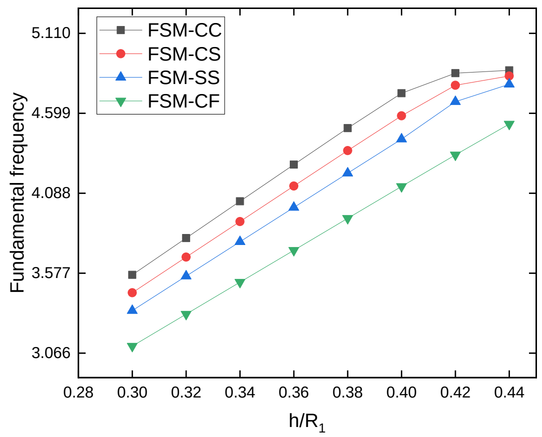

(d) against nonlocal parameter e_0a=0.40 with R_1=1.5 nm

Fig. 3 Influence of diverse boundary conditions on chiral double-walled CNT (8, 3)

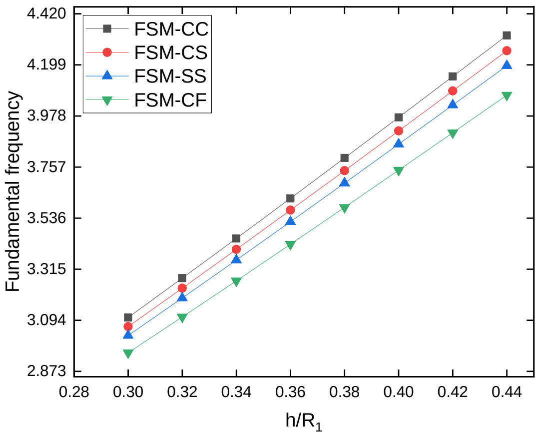

(a) against nonlocal parameter e_0a=0.18 with R_1=0.35 nm

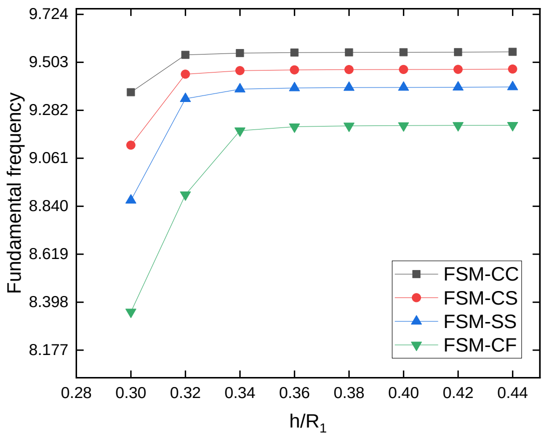

(b) against nonlocal parameter e_0a=0.18 with R_1=1.5 nm

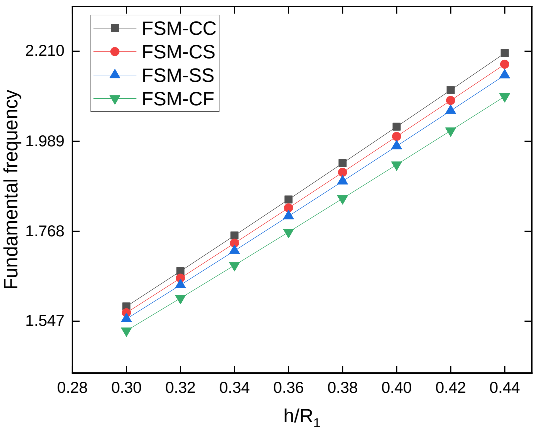

(c) against nonlocal parameter e_0a=0.40 with R_1=0.35 nm

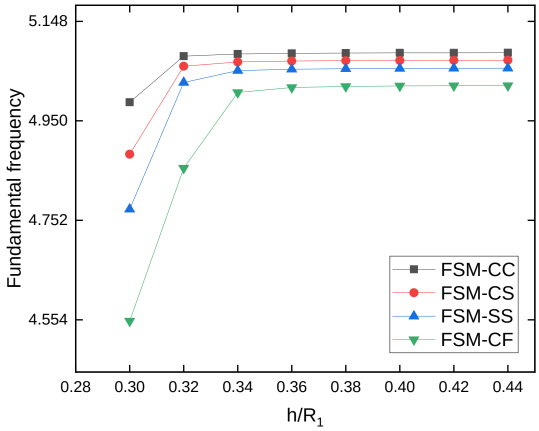

(d) against nonlocal parameter e_0a=0.40 with R_1=1.5 nm

Fig. 4 Influence of diverse boundary conditions on chiral double-walled CNT (11, 4)

CNT as: $\xi = \omega R\sqrt{(1-\nu^2)\rho / E}$. The obtained results are cross-compared with external data and provide agreement between modeling, computation and experimental outcomes as shown in Tables 1 and 2. Fig. 2 plots the fundamental frequency versus ***L/d*** for FSM-CC end condition for different modes of vibration. It should be mentioned for both cases, the values of *L/d* varies from 4.67 ~ 35.34. It is found that from Fig. 3, that frequencies of first (1, 1) and third (3, 1) vibration modes decrease and reaches the constant values on increasing of ***L/d***. The influence of ***L/d*** on the frequency of present model has been discussed and checked with MD simulation as shown in Fig. 3 for FSM-CC end condition.

The obtained results are well agreed with the reported results of MD simulation (Zhang *et al.* 2009). Particularly, the frequencies (THz) of double-walled CNTs correspond to *L/d*=6.71 are 0.671, 1.565, 2.552, 3.523 for present model and 0.681, 1.535, 2.536, 3.588, as given by Duan *et al.* (2007), respectively. The vibrations of FSM-CC double-walled CNTs have been investigated both by simulations techniques (Li and Chou 2003, Li and Chou 2004, Zhang *et al.* 2009) and experimentally (Yakobson *et al.* 1996, Hsu *et al.* 2008). It is seen that the frequencies have a notable effect on the vibration of double-walled CNTs with shorter length-to-diameter ratio. Fig. 3 exhibits the variation of fundamental eigen frequencies against two distinct values of nonlocal parameter e_0a=0.18, 0.40 for chiral (8, 3) double-walled CNTs. The detail inspection of aspect ratio thickness to radius (h/R_1) that ranges from 0.30nm to 0.44 nm is discussed subject to four boundary conditions FSM-CC, FSM-CS, FSM-SS and FSM-CF. The radius of inner tube is considered as R_1=0.35 nm and R_1=1.5 nm with all above mentioned numerical estimates of physical parameters incorporating also with *vdW* interaction between two tubes of double-walled CNTs. The graph in figure shows that with an increase in values of aspect ratio, frequency corresponding to each boundary condition tends to increase. For lessen value of e_0a the frequencies are higher for FSM-CC, FSM-CS, FSM-SS and FSM-CF respectively. Whereas for lower aspect ratio the frequencies coincide but as it continues to expand the difference between all respective boundary conditions slightly tend to increase. One of main findings depicted by graph is that calculated frequencies coincide for all boundary condition in beginning and continue to ascent with a rise in aspect ratio.

On the other hand chiral (8, 3) with R_1=1.5 nm attains higher frequencies for distinct values of nonlocal parameters compared to R_1=0.35 nm. The rooted nonlocal elasticity model also produces more significant results for minimal radius of tubes. The graphs in Fig. 4 compares the fundamental frequencies of chiral (11, 4) with inner radius R_1=0.35 nm and R_1=1.5 nm. The all other numerical

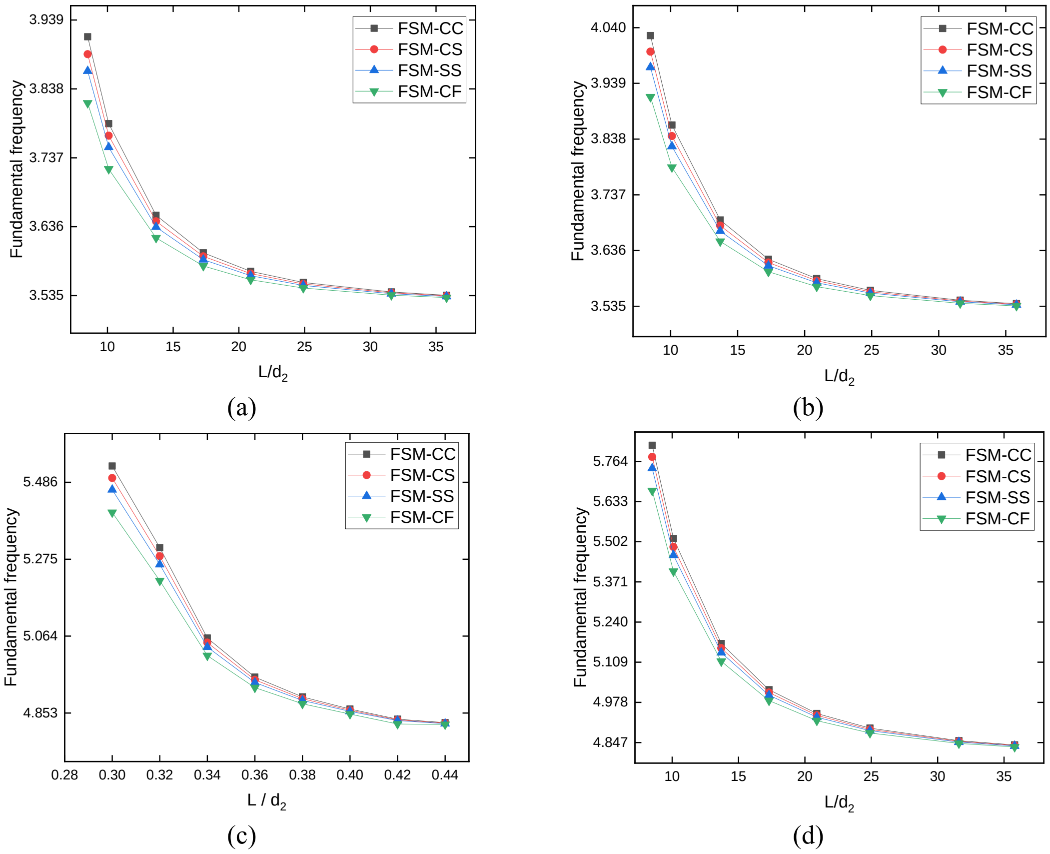

Fig. 5 Influence of diverse boundary conditions on chiral double-walled CNT (8, 3), (9, 3), (11, 4) and (13, 4) with R_1=0.35 nm against nonlocal parameter e_0a=0.18 displaying the comparison of aspect ratio L/d

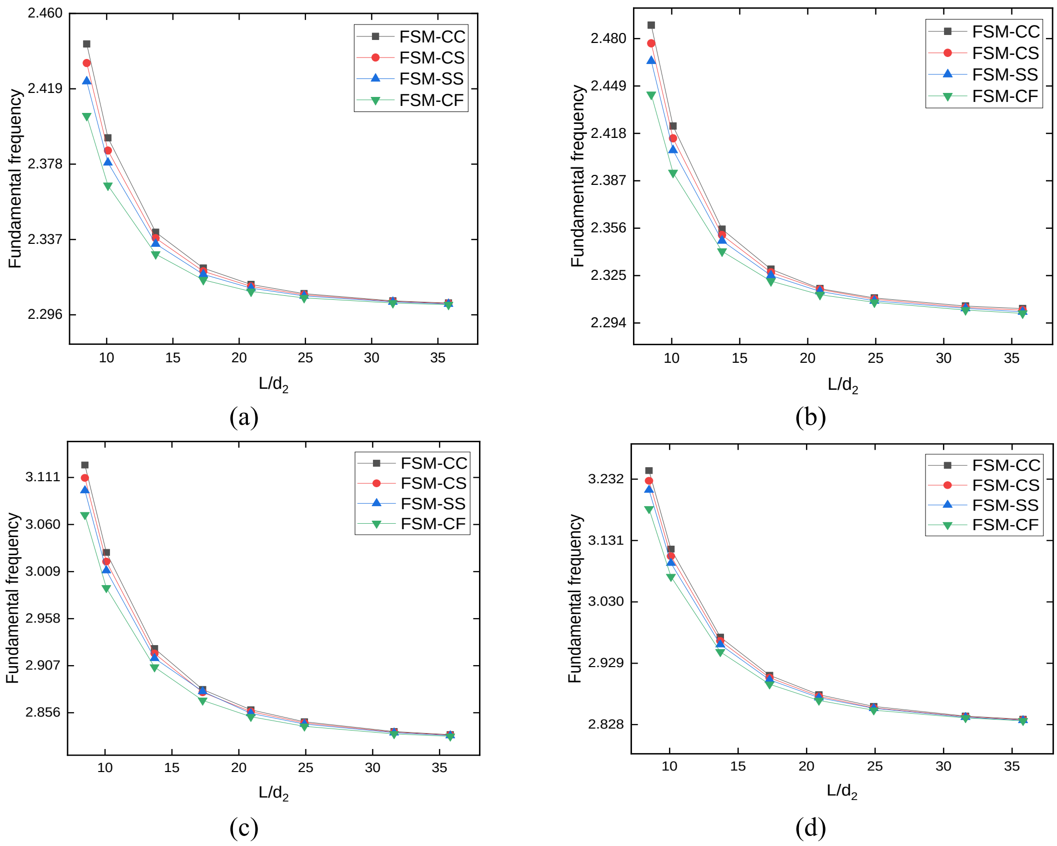

Fig. 6 Influence of diverse boundary conditions on chiral double-walled CNT (8, 3), (9, 3) ,(11, 4) and (13, 4) with R_1=0.35 nm against nonlocal parameter e_0a=0.40 displaying the comparison of aspect ratio L/d

estimates are same as quoted above. The curves in graphs shows the validity of small-scale effect as the frequencies decrease with an increase of nonlocal parameter. Also, it is observed that as inner radius is reduced so the fundamental frequencies possess more significant result. The FSM-CC attains highest fundamental frequency chased by FSM-CS after that FSM-SS and at last FSM-CF comes. In both figures smaller inner radius shows insignificance of boundary conditions for low aspect ratio. For the special case, in Fig. 4(b) and (d) for chiral (11, 4), in start the frequency rises with jump for all corresponding end supports, but as aspect ratio expands it displays an infinitesimal increase respectively. The graphs in Fig. 5 included the fundamental frequencies of chiral (8, 3), (9, 4), (11, 4) and (13, 4) showing diversity with the e_0a=0.18. The all depicted frequencies in graphs are facing length to diameter ratio(ranges from 8 nm to 35 nm). It is noticed that there is uniform decrease in frequencies of chiral corresponding to all four conditions FSM-CC, FSM-CS, FSM-SS and FSM-CF. In Fig. 5, the inner tube radius is taken as R_1=0.35 nm with other estimates remained same. Fig. 5 display the comparison chiral (7, 0) with e_0a=0.18. It is obviously seen there is an decreasing trend and which remains unchanged for all boundary conditions as well as chiral double-walled CNTs with distinct indices possess the identical behavior. It is noticeable that chiral (13, 4) procure the higher frequency in comparison of L/d_2 for chiral (8, 3), (9, 3) and (11, 4) against nonlocal parameter. The graph in Fig. 5(a) represented the frequency 3.9144 against the first thickness to radius ratio for FSM-CC of chiral (8, 3), whereas in Fig. 5(d) it was espied as 5.8167. Fig. 6 illustrates the influence of boundary conditions for chiral (8, 3), (9, 3), (11, 4) and (13, 4) respectively considering the e_0a=0.40. The drop of the curves opposite of length to diameter ratio affirms the nonlocal effect. Corresponding to all chiral frequencies, there is seen drop in the frequencies as inflates the nonlocal parameter value. Also, as enlarges the indices of chiral, the curves indicated escalation in frequencies and the pattern recognized the fact. The gap presented in four boundary conditions is obvious in start of the curves as FSM-CF secures the lowest frequency in comparison of FSM-SS, FSM-CS and FSM-CC. Moreover, the more accretion in the nonlocal parameter, the lower the fundamental frequencies are observed. It shows a descent in fundamental frequencies with an ascent in nonlocal parameter. However the validation of present model is evidently observed by meeting all four end supports at end with the increase in tube's length.

5. Conclusions

The Flügge shell theory based on nonlocal elasticity investigates the vibration characteristics of double-walled CNTs. Theoretical formation of the nonlocal model involves the van der Waals interactions between the tubes and impact of small-scale effect subjected to four boundary supports. The wave propagation approach is exercised to determine eigen frequencies for chiral CNTs. The fundamental frequencies scrutinized with assorted length to diameter ratio and thickness to radius ratio. The analysis done with the findings

• The rise in value of nonlocal parameter reduces the corresponding fundamental frequency estimates.
• Due to small scale effect fundamental frequency ratio decreases as length to diameter ratio increases.
• Small scale effect becomes more pronounced on all end supports for the higher values of aspect ratio (length to diameter).
• With the large inner tube radius double-walled CNTs behaves more sensitive towards nonlocal parameter.
• An increase in indices of chiral double-walled CNTs with increasing inner tube radius become insignificant for thickness to radius ratio.

The present study can be appropriate to employ for analyzing the vibrations in double-walled CNTs with Galerkin and finite element methods.

Declaration of conflicting interests

The author(s) declared no potential conflicts of interest with respect to the research, authorship, and/or publication of this article.

References

Adela, I. (2018), *Computational Fluid Dynamics*, Romania.

Amara, K., Tounsi, A., Mechab, I. and Adda-Bedia, E.A. (2010), "Nonlocal elasticity effect on column buckling of multiwalled carbon nanotubes under temperature field", *Appl. Math. Model.*, **34**(12), 3933-3942. https://doi.org/10.1016/j.apm.2010.03.029.

Ansari, R. and Rouhi, H. (2012), "Nonlocal analytical Flügge shell model for the axial buckling of double-walled carbon nanotubes with different end conditions", *Int. J. Nano*, **7**, 1250081. https://doi.org/10.1142/S179329201250018X.

Ansari, R. and Rouhi, H. (2013), "Nonlocal analytical Flügge shell model for the vibrations of double-walled carbon nanotubes with different end conditions", *Int. J. Appl. Mech.*, **80**, 021006-1. https://doi.org/10.1142/S179329201250018X.

Ansari, R., Hemmatnezhad, M. and Rezapour, J. (2011), "The thermal effect on nonlinear oscillations of carbon nanotubes with arbitrary boundary conditions", *Curr. Appl. Phys.*, **11**(3), 692-697. https://doi.org/10.1016/j.cap.2010.11.034.

Ansari, R., Sahmani, S. and Arash, B. (2010), "Nonlocal plate model for free vibrations of single-layered graphene sheets", *Phys. Lett. A.*, **375**(1), 53-62. https://doi.org/10.1016/j.physleta.2010.10.028.

Arefi, M. and Zenkour, A.M. (2018), "Size-dependent thermoelastic analysis of a functionally graded nanoshell", *Mod. Phys. Lett. B*, **32**(3), 1850033. https://doi.org/10.1142/S0217984918500331.

Arefi, M., Bidgoli, E.M.R. and Rabczuk, T. (2019), "Effect of various characteristics of graphene nanoplatelets on thermal buckling behavior of FGRC micro plate based on MCST", *Eur. J. Mech.-A/Solid.*, **77**, 103802. https://doi.org/10.1016/j.euromechsol.2019.103802.

Arefi, M., Bidgoli, E.M.R. and Rabczuk, T. (2019), "Thermo-mechanical buckling behavior of FG GNP reinforced micro plate based on MSGT", *Thin Wall. Struct.*, **142**, 444-459. https://doi.org/10.1016/j.tws.2019.04.054.

Arefi, M., Bidgoli, E.M.R., Dimitri, R. and Tornabene, F. (2018), "Free vibrations of functionally graded polymer composite nanoplates reinforced with graphene nanoplatelets", *Aerosp. Sci. Technol.*, **81**, 108-117. https://doi.org/10.1016/j.ast.2018.07.036.

Arefi, M., Bidgoli, E.M.R., Dimitri, R., Bacciocchi, M. and Tornabene, F. (2019), "Nonlocal bending analysis of curved nanobeams reinforced by graphene nanoplatelets", *Compos. Part B: Eng.*, **166**, 1-12. https://doi.org/10.1016/j.compositesb.2018.11.092.

Arefi, M., Karroubi, R. and Irani-Rahaghi, M. (2016), "Free vibration analysis of functionally graded laminated sandwich cylindrical shells integrated with piezoelectric layer", *Appl. Math. Mech.*, **37**(7), 821-834. https://doi.org/10.1007/s10483-016-2098-9.

Arefi, M., Mohammadi, M., Tabatabaeian, A., Dimitri, R. and Tornabene, F. (2018), "Two-dimensional thermo-elastic analysis of FG-CNTRC cylindrical pressure vessels", *Steel Compos. Struct.*, **27**(4), 525-536. https://doi.org/10.12989/scs.2018.27.4.525.

Ayat, H., Kellouche, Y., Ghrici, M. and Boukhatem, B. (2018), "Compressive strength prediction of limestone filler concrete using artificial neural networks", *Adv. Comput. Des.*, **3**(3), 289-302. https://doi.org/10.12989/acd.2018.3.3.289.

Batou, B., Nebab, M., Bennai, R., Atmane, H.A., Tounsi, A. and Bouremana, M. (2019), "Wave dispersion properties in imperfect sigmoid plates using various HSDTs", *Steel Compos. Struct.*, **33**(5), 699. https://doi.org/10.12989/scs.2019.33.5.699.

Behera, S. and Kumari, P. (2018), "Free vibration of Levy-type rectangular laminated plates using efficient zig-zag theory", *Adv. Comput. Des.*, **3**(3), 213-232. https://doi.org/10.12989/acd.2018.3.3.213.

Benguediab, S., Tounsi, A., Zidour, M. and Semmah, A. (2014), "Chirality and scale effects on mechanical and buckling properties of zigzag double-walled carbon nanotubes", *Compos. Part B*, **57**, 21-24. https://doi.org/10.1016/j.compositesb.2013.08.020.

Bouadi, A., Bousahla, A.A., Houari, M.S.A., Heireche, H. and Tounsi, A. (2018), "A new nonlocal HSDT for analysis of stability of single layer graphene sheet", *Adv. Nano Res.*, **6**(2), 147-162. https://doi.org/10.12989/anr.2018.6.2.147.

Brischotto, S. (2015), "A continuum shell model including van der Waals interaction for free vibrations of double-walled carbon nanotubes", *CMES*, **104**, 305-327.

Dehsaraji, M.L., Arefi, M. and Loghman, A. (2020), "Size dependent free vibration analysis of functionally graded piezoelectric micro/nano shell based on modified couple stress theory with considering thickness stretching effect", *Defence Technology*. https://doi.org/10.1016/j.dt.2020.01.001.

Dehsaraji, M.L., Arefi, M. and Loghman, A. (2020), "Three dimensional free vibration analysis of functionally graded nano cylindrical shell considering thickness stretching effect", *Steel Compos. Struct.*, **34**(5), 657-670. https://doi.org/10.12989/scs.2020.34.5.657.

Do, Q.C., Pham, D.N., Vu, D.Q., Vu, T.T.A. and Nguyen, D.D. (2019), "Nonlinear buckling and post-buckling of functionally graded CNTs reinforced composite truncated conical shells subjected to axial load", *Steel Compos. Struct.*, **31**(3), 243-259. https://doi.org/10.12989/scs.2019.31.3.243.

Eringen, A.C. (1983), "On differential equations of nonlocal elasticity and solutions of screw dislocation and surface waves", *J. Appl. Phys.*, **54**, 4703-4710. https://doi.org/10.1063/1.332803.

Eringen, A.C. (2002), *Nonlocal Continuum Field Theories*, Science and Business Media, New York.

Fakhrabadi, M.M.S., Rastgoo, A. and Ahmadian, M.T. (2015), "Application of electrostatically actuated carbon nanotubes in nanofluidic and bio-nanofluidic sensors and actuators", *Measure.*, **73**, 127-136. https://doi.org/10.1016/j.measurement.2015.05.009.

Flügge, W. (1962), *Statik und Dynamik der Scahlen*, Springer, Berlin, Germany.

Fu, Y.M., Hong, J.W. and Wang, X.Q. (2006), "Analysis of nonlinear vibration for embedded carbon nanotubes", *J. Sound Vib.*, **296**(4-5), 746-756. https://doi.org/10.1016/j.jsv.2006.02.024.

Hao, M.J., Guo, X.M. and Wang, Q. (2010), "Small-scale effect on torsional buckling of multi-walled carbon nanotubes", *Eur. J. Mech. A/Solid.*, **29**(1), 49-55. https://doi.org/10.1016/j.euromechsol.2009.05.008.

Hernandez, E., Goze, C., Bemier, P. and Rubio, A. (1998), "Elastic properties of C and BxCyNz composite nanotubes", *Phys. Rev. Lett.*, **80**, 4502-505. https://doi.org/10.1103/PhysRevLett.80.4502.

Heydarpour, Y., Aghdam, M.M. and Malekzadeh, P. (2014), "Free vibration analysis of rotating functionally graded carbon nanotube-reinforced composite truncated conical shells", *Compos. Struct.*, **117**, 187-200. https://doi.org/10.1016/j.compstruct.2014.06.023.

Hsu, J.C., Chang, R.P. and Chang, W.J. (2008), "Resonance frequency of chiral single-walled carbon nanotubes using Timoshenko beam theory", *Phys. Lett. A*, **372**(16), 2757-2759. https://doi.org/10.1016/j.physleta.2008.01.007.

Hu, Y.G., Liew, K.M., Wang, Q., He, X.Q. and Yakobson, B.I. (2008), "Nonlocal shell model for elastic wave propagation in single- and double-walled carbon nanotubes", *J. Mech Phys. Solid.*, **56**, 3475-3485. https://doi.org/10.1016/j.jmps.2008.08.010.

Hussain, M. and Naeem, M.N. (2019a), "Rotating response on the vibrations of functionally graded zigzag and chiral single walled carbon nanotubes". *Appl. Math. Model.*, **75**, 506-520. https://doi.org/10.1016/j.apm.2019.05.039.

Hussain, M. and Naeem, M.N. (2019b), "Effects of ring supports on vibration of armchair and zigzag FGM rotating carbon nanotubes using Galerkin's method", *Compos. Part B: Eng.*, **163**, 548-561. https://doi.org/10.1016/j.compositesb.2018.12.144.

Iijima, S. (1991), "Helical microtubules of graphitic carbon", *Nature*, **354**(1), 56-58. https://doi.org/10.1038/354056a0.

Iijima, S., Brabec, C., Maiti, A. and Bemholc, J. (1996), "Structural flexibility of carbon nanotubes", *J. Chem. Phys.*, **104**(5), 2089-2092. https://doi.org/10.1063/1.470966.

Jamali, M., Shojaee, T., Mohammadi, B. and Kolahchi, R. (2019), "Cut out effect on nonlinear post-buckling behavior of FG-CNTRC micro plate subjected to magnetic field via FSDT", *Adv. Nano Res.*, **7**(6), 405-417. https://doi.org/10.12989/anr.2019.7.6.405.

Ke, L.L., Xiang, Y., Yang, J. and Kitipornchai, S. (2009), "Nonlinear free vibration of embedded double-walled carbon nanotubes based on nonlocal Timoshenko beam theory", *Comput. Mater. Sci.*, **47**(2), 409-417. https://doi.org/10.1016/j.commatsci.2009.09.002.

Khosrazadeh, A. and Hajabasi, M.A. (2012), "Free vibrations of embedded doube-walled carbon nanotubes considering nonlinear interlayer van der Waals forces", *J. AMP*, **36**, 997-1007. https://doi.org/10.1016/j.apm.2011.07.063.

Lei, Z. and Zhang, Y. (2018), "Characterizing buckling behavior of matrix-cracked hybrid plates containing CNTR-FG layers", *Steel Compos. Struct.*, **28**(4), 495-508. https://doi.org/10.12989/scs.2018.28.4.495.

Li, C. and Chou, T.W. (2003), "A structural mechanics approach for the analysis of carbon nanotubes", *Int. J. Solid. Struct.*, **40**(10), 2487-2492. https://doi.org/10.1016/S0020-7683(03)00056-8.

Loy, C.T. Lam, K.Y. and Reddy, J.N. (1999), "Vibration of functionally graded cylindrical shells", *Int. J. Mech. Sci.*, **41**, 309-324. https://doi.org/10.1016/S0020-7403(98)00054-X.

Moradi-Dastjerdi, R. and Payganeh, G. (2017), "Transient heat transfer analysis of functionally graded CNT reinforced cylinders with various boundary conditions", *Steel Compos. Struct.*, **24**, 359-367. https://doi.org/10.12989/scs.2017.24.3.359.

Narwariya, M., Choudhury, A. and Sharma, A.K. (2018), "Harmonic analysis of moderately thick symmetric cross-ply laminated composite plate using FEM", *Adv. Comput. Des.*, **3**(2), 113-132. https://doi.org/10.12989/acd.2018.3.2.113.

Natsuki, T., Morinobu, E. andTsuda, H. (2006), "Vibration analysis of embedded carbon nanotubes using wave propagation approach", *J. Appl. Phys*., **99**(3), 034311. https://doi.org/10.1063/1.2170418.

Natsuki, T., Qing, Q.N. and Morinobu, E. (2007), "Wave propagation in single-walled and double-walled carbon nanotubes filled with fluids", *J. Appl. Phys*., **101**(3), 034319-034319-5. https://doi.org/10.1063/1.2432025.

Peddieson, J., Buchanan, G.R. and McNitt, R.P. (2003), "Application of nonlocal continuum models to nanotechnology", *Int. J. Eng. Sei*., **41**, 305-312. https://doi.org/10.1016/S0020-7225(02)00210-0.

Pradhan, S.C. and Phadikar, J.K. (2009), "Small scale effect on vibration of embedded multilayered graphene sheets based on nonlocal continuum models", *Phys. Lett. A*., **373**(11), 1062-9. https://doi.org/10.1016/j.physleta.2009.01.030.

Qian, D., Wagner, G.J., Liu, W.K., Yu, M.F. and Ruoff, R.S. (2002), "Mechanics of carbon nanotubes", *Appl. Mech. Rev.*, **55**(6), 495-533. https://doi.org/10.1115/1.1490129.

Rouhi, H., Ansari, R. and Arash, B. (2013), "Vibration analysis of double-walled carbon nanotubes based on the non-local donnell shell via a new numerical approach", *Int J. Mech. Sei*., **37**, 91-105.

Rouhi, H., Bazdid Vahdati, M. and Ansari, R. (2015), "Rayleigh-Rits vibrational analysis of multi-walled carbon nanotubes based on the non-local Flugge shell theory", *J. Compos*., 750392. https://doi.org/10.1155/2015/750392.

Salah, F., Boucham, B., Bourada, F., Benzair, A., Bousahla, A.A. and Tounsi, A. (2019), "Investigation of thermal buckling properties of ceramic-metal FGM sandwich plates using 2D integral plate model", *Steel Compos. Struct.*, **33**(6), 805. https://doi.org/10.12989/scs.2019.33.6.805.

Sanchez-Portal, D., Artacho, E., Soler, J.M., Rubio, A. and Ordejón, P. (1999), "Ab-initio structural, elastic, and vibrational properties of carbon nanotubes", *Phys. Rev. B*, **59**, 12678-2688. http://dx.doi.org/10.1103/PhysRevB.59.12678.

Sedighi, H.M. and Yaghootian, A. (2016), "Dynamic instability of vibrating carbon nanotubes near small layers of graphite sheets based on nonlocal continuum elasticity", *J. Appl. Mech. Techn. Phys*., **57**(1), 90-100. https://doi.org/10.1134/S0021894416010107.

Sedighi, H.M., Reza, A. and Zare, J. (2011)", Study on the frequency-amplitude relation of beam vibration", *Int. J. Phys. Sci.*, **6**(36), 8051-8056. https://doi.org/10.5897/IJPS11.1556.

Shafiei, H. and Setoodeh, A.R. (2017), "Nonlinear free vibration and post-buckling of FG-CNTRC beams on nonlinear foundation", *Steel Compos. Struct.*, **24**(1), 65-77. https://doi.org/10.12989/scs.2017.24.1.065.

She, G.L., Ren, Y.R. and Yuan, F.G. (2019), "Hygro-thermal wave propagation in functionally graded double-layered nanotubes systems", *Steel Compos. Struct.*, **31**(6), 641-653. https://doi.org/10.12989/scs.2019.31.6.641.

Shen, H.S. and Zhang, C.L. (2010), "Torsional buckling and post buckling of double-walled carbon nanotubes by nonlocal shear deformable shell model", *Compos. Struct*., **92**(5), 1073-1084. https://doi.org/10.1016/j.compstruct.2009.10.002.

Soldano, C. (2015), "Hybrid metal-based carbon nanotubes", "Novel platform for multifunctional applications", *Prog. Mater. Sci.*, **69**, 183-212. https://doi.org/10.1016/j.pmatsci.2014.11.001.

Sosa, E.D., Darlington, TK., Hanos, B.A. and O'Rourke, M.J.E. (2014), "Multifunctional thermally remendable nanocomposites", *J. Compos*., Article ID 705687, 12. http://dx.doi.org/10.1155/2014/705687.

Sudak, L.J. (2003), "Column buckling of multi-walled carbon nanotubes using nonlocal continuum mechanics", *J. Appl. Phys*., **94**, 7281-7287. https://doi.org/10.1063/1.1625437.

Tahouneh, V. (2017), "Effects of CNTs waviness and aspect ratio on vibrational response of FG-sector plate", *Steel Compos. Struct.*, **25**(6), 649-661. https://doi.org/10.12989/scs.2017.25.6.649.

Usuki, T. and Yogo, K. (2009), "Beam equations for multi-walled carbon nanotubes derived from Flugge shell theory", *Proc. Royal Soc. A*., **465**(2104), 1199-1226. https://doi.org/10.1098/rspa.2008.0394.

Vodenitcharova, T. and Zhang, L.C. (2003), "Effective wall thickness of single walled carbon nanotubes", *Phys. Rev. B*, **68**, 165401. https://doi.org/10.1103/PhysRevB.68.165401.

Wang, C.Y. and Zhang, L.C. (2007), "Modelling the free vibration of single-walled carbon nanotubes", *Proceedings of the 5th Australasian Congress on Applied Mechanics*, Engineers Australia.

Wang, Q., Varadan, V.K. and Quek, S.T. (2006), "Small scale effect on elastic buckling of carbon nanotubes with nonlocal continuum models", *Phys. Lett. A*., **357**(2), 130-135. https://doi.org/10.1016/j.physleta.2006.04.026.

Wang, Q., Zhou, G.Y. and Lin, K.C. (2006), "Scale effect on wave propagation of double-walled carbon nanotubes", *Int. J. Solid. Struct*., **43**, 6071-6084. https://doi.org/10.1016/j.ijsolstr.2005.11.005.

Xiaobin, L., Shuangxi, X., Weiguo, W. and Jun, L. (2014), "An exact dynamic stiffness matrix for axially loaded double-beam systems", *Sadhana*, **39**(3), 607-623. https://doi.org/10.1007/s12046-013-0214-5.

Xu, K.U., Aifantis, E.C. and Yan, Y.H. (2008), "Vibrations of double-walled carbon nanotubes with different boundary conditions between inner and outer tubes", *J. Appl. Mech*., **75**(2), 021013-1. https://doi.org/10.1115/1.2793133.

Yakobson, B.I., Brabec, C.J. and Bernholc, J. (1996), "Nano-mechanics of carbon tubes: instabilities beyond linear response", *Phys. Rev. Lett*., **76**, 2511-2514. https://doi.org/10.1103/PhysRevLett.76.2511.

Yakobson, B.I., Campbell, M.P., Brabec, C.J. and Bemholc J. (1997), "High strain rate fracture and C-chain unravelling in carbon nanotubes", *Comput. Mater. Sei*., **8**(4), 341-348. https://doi.org/10.1016/S0927-0256(97)00047-5.

Yazdani, R. and Mohammadimehr, M. (2019), "Double bonded Cooper-Naghdi micro sandwich cylindrical shells with porous core and CNTRC face sheets: Wave propagation solution", *Comput. Concrete*, **24**(6), 499-511. https://doi.org/10.12989/cac.2019.24.6.499.

Yoon, J., Ru, C.Q. and Mioduchowski, A. (2003), "Vibration of an embedded multiwall carbon nanotube", *Compos. Sei. Tech*., **63**(11), 1533-1542. https://doi.org/10.1016/S0266-3538(03)00058-7.

Youcef, D.O., Kaci, A., Benzair, A., Bousahla, A.A. and Tounsi, A. (2018), "Dynamic analysis of nanoscale beams including surface stress effects", *Smart Struct. Syst*., **21**(1), 65-74. https://doi.org/10.12989/sss.2018.21.1.065.

Zemri, A., Houari, M.S.A., Bousahla, A.A. and Tounsi, A. (2015), "A mechanical response of functionally graded nanoscale beam: an assessment of a refined nonlocal shear deformation theory beam theory", *Struct. Eng. Mech*., **54**(4), 693-710. http://dx.doi.org/10.12989/sem.2015.54.4.693.

Zhang, Y., Li, G. and Liew, K.M. (2018), "Thermomechanical buckling characteristic of ultrathin films based on nonlocal elasticity theory", *Compos. Part B: Eng.*, **153**, 184-193. https://doi.org/10.1016/j.compositesb.2018.07.046.

CC

Appendix-I

$$g_{11}{}^{(i)}=\frac{Eh}{1-\nu^2}\frac{\partial^2}{\partial x^2}+\frac{1}{R_i^2}\frac{Eh}{2(1+\nu)}\frac{\partial^2}{\partial\theta^2}$$

$$g_{12}{}^{(i)}=\frac{1}{R_i}\left(\frac{Eh\nu}{1-\nu^2}+\frac{Eh}{2(1+\nu)}\right)\frac{\partial^2}{\partial\theta\partial x}$$

$$g_{13}{}^{(i)}=\frac{1}{R_i}\frac{Eh\nu}{1-\nu^2}\frac{\partial}{\partial x}$$

$$g_{21}{}^{(i)}=g_{12}{}^{(i)}$$

$$g_{22}{}^{(i)}=\left(\frac{Eh}{2(1+\nu)}+\frac{D(1-\nu)}{R_i^2}\right)\frac{\partial^2}{\partial x^2}+\frac{1}{R_i^2}\left(\frac{Eh}{1-\nu^2}+\frac{D}{R_i^2}\right)\frac{\partial^2}{\partial\theta^2}$$

$$g_{23}{}^{(i)}=-\frac{D}{R_i^2}\frac{\partial^3}{\partial x^2\partial\theta}-\frac{\nu D}{R_i^4}\frac{\partial^3}{\partial\theta^3}+\frac{1}{R_i^2}\frac{Eh}{1-\nu^2}\frac{\partial}{\partial\theta}$$

$$g_{31}{}^{(i)}=-g_{13}{}^{(i)}$$

$$g_{32}{}^{(i)}=\frac{D}{R_i^2}(2-\nu)\frac{\partial^3}{\partial x^2\partial\theta}+\frac{D}{R_i^4}\frac{\partial^3}{\partial\theta^3}-\frac{1}{R_i^2}\frac{Eh}{1-\nu^2}\frac{\partial}{\partial\theta}$$

$$g_{33}{}^{(i)}=-D\frac{\partial^4}{\partial x^4}-\frac{2D}{R_i^2}\frac{\partial^4}{\partial x^2\partial\theta^2}-\frac{D}{R_i^4}\frac{\partial^4}{\partial\theta^4}-\frac{1}{R_i^2}\frac{Eh}{1-\nu^2}$$

Appendix-II

$$G_{11}{}^{(i)}=\frac{Eh}{1-\nu^2}(-k_m{}^2)+\frac{1}{R_i^2}\frac{Eh}{2(1+\nu)}(-n^2)$$

$$G_{12}{}^{(i)}=\frac{1}{R_i}\left(\frac{Eh\nu}{1-\nu^2}+\frac{Eh}{2(1+\nu)}\right)(-nik_m)$$

$$G_{13}{}^{(i)}=\frac{1}{R_i}\frac{Eh\nu}{1-\nu^2}(-ik_m) \qquad G_{21}{}^{(i)}=-G_{12}{}^{(i)}$$

$$G_{22}{}^{(i)}=\left(\frac{Eh}{2(1+\nu)}+\frac{D(1-\nu)}{R_i^2}\right)(-k_m{}^2)$$

$$+\frac{1}{R_i^2}\left(\frac{Eh}{1-\nu^2}+\frac{D}{R_i^2}\right)(-n^2)$$

$$G_{23}{}^{(i)}=-\frac{D}{R_i^2}(nk_m{}^2)-\frac{\nu D}{R_i^4}n^3+\frac{1}{R_i^2}\frac{Eh}{1-\nu^2}(-n)$$

$$G_{31}{}^{(i)}=-G_{13}{}^{(i)}$$

$$G_{32}{}^{(i)}=\frac{D}{R_i^2}(2-\nu)(-nk_m{}^2)-\frac{D}{R_i^4}n^3-\frac{1}{R_i^2}\frac{Eh}{1-\nu^2}n$$

$$G_{33}{}^{(i)}=-Dk_m{}^4-\frac{2D}{R_i^2}n^2k_m{}^2-\frac{D}{R_i^4}n^4-\frac{1}{R_i^2}\frac{Eh}{1-\nu^2}$$